Supplementary File of 'Efficient Resource Allocation in Cooperative Co-evolution for Large-scale Global Optimization'

Ming Yang, Mohammad Nabi Omidvar, Changhe Li, *Member, IEEE*, Xiaodong Li, *Senior Member, IEEE*, Zhihua Cai, Borhan Kazimipour, and Xin Yao, *Fellow, IEEE*

CONTENTS

The work was supported in part by the National Natural Science Foundation of China (Grant Nos. 61305086, 61673355, 61673354, 61329302 and 61305079) and EPSRC (Grant No. EP/K001523/1). *(Corresponding author: Xin Yao.)*

M. Yang and Z. Cai are with the School of Computer Science, China University of Geosciences, Wuhan, 430074, China. M. Yang and Z. Cai are also with the Hubei Key Laboratory of Intelligent Geo-Information Processing, China University of Geosciences, Wuhan 430074, China (e-mail: yangming0702@gmail.com, zhcai@cug.edu.cn).

C. Li is with the School of Automation, China University of Geosciences, Wuhan, 430074, China (e-mail: changhe.lw@gmail.com).

M. N. Omidvar and X. Yao are with the Centre of Excellence for Research in Computational Intelligence and Applications, School of Computer Science, University of Birmingham, Birmingham B15 2TT, U.K. X. Yao is also with Department of Computer Science and Engineering, Southern University of Science and Technology, Shenzhen, 518055, China. (e-mail: m.omidvar@cs.bham.ac.uk, x.yao@cs.bham.ac.uk).

X. Li and B. Kazimipour are with the School of Computer Science and Information Technology, RMIT University, Melbourne, VIC 3001, Australia (e-mail: xiaodong.li@rmit.edu.au, borhan.kazimipour@rmit.edu.au).

TABLE I: The average fitness values ± standard deviations on the CEC'2010 and CEC'2013 functions over 25 independent runs. The significantly better results are in bold font (Wilcoxon rank sum test with Holm p-value correction, α=0.05). R^+, R^- and p-value are obtained through multiple-problem analysis by the Wilcoxon test between CCFR-I (U=D_i) and its competitors.

CEC'2010 Functions			
F	CCFR-I ($U = D_i$)	CCFR-I ($U = 2D_i$)	CCFR-I ($U = 10D_i$)
f_1	1.20e-05±4.89e-06	1.31e-05±5.19e-06	1.68e-05±6.54e-06↑
f_2	**2.75e+01±5.25e+00**	5.13e+01±5.04e+00↑	1.52e+02±7.22e+00↑
f_3	**4.56e+00±4.63e-01**	5.56e+00±4.63e-01↑	8.10e+00±4.65e-01↑
f_4	8.33e+10±6.16e+10	8.69e+10±4.68e+10	1.06e+11±4.31e+10↑
f_5	7.23e+07±1.32e+07	7.32e+07±1.22e+07	9.12e+07±1.74e+07↑
f_6	7.74e+05±7.15e+05	7.83e+05±8.28e+05	7.28e+05±8.51e+05
f_7	**1.49e-03±2.47e-04**	1.66e-03±2.78e-04↑	2.14e-03±3.90e-04↑
f_8	3.19e+05±1.08e+06	6.38e+05±1.46e+06	9.57e+05±1.70e+06↑
f_9	9.38e+06±1.18e+06	8.81e+06±1.05e+06	1.05e+07±1.44e+06↑
f_{10}	1.41e+03±1.01e+02	1.42e+03±7.83e+01	1.61e+03±1.10e+02↑
f_{11}	1.03e+01±2.71e+00	9.72e+00±2.11e+00	1.00e+01±2.59e+00
f_{12}	**1.17e+00±4.57e+00**	4.72e+00±1.75e+01↑	7.49e+00±2.30e+01↑
f_{13}	3.18e+02±9.91e+01	3.25e+02±1.01e+02	4.03e+02±9.45e+01↑
f_{14}	2.48e+07±2.85e+06	2.48e+07±2.85e+06	2.48e+07±2.85e+06
f_{15}	2.81e+03±1.31e+02	2.81e+03±1.31e+02	2.81e+03±1.31e+02
f_{16}	2.01e+01±2.62e+00	2.01e+01±2.62e+00	2.01e+01±2.62e+00
f_{17}	9.78e+00±1.09e+01	9.78e+00±1.09e+01	9.78e+00±1.09e+01
f_{18}	1.14e+03±1.82e+02	1.14e+03±1.82e+02	1.14e+03±1.82e+02
f_{19}	1.16e+06±9.47e+04	1.16e+06±9.47e+04	1.16e+06±9.47e+04
f_{20}	1.01e+09±8.96e+08	1.01e+09±8.96e+08	1.01e+09±8.96e+08
R^+	—	168.0	170.0
R^-	—	42.0	40.0
p-value	—	2.66e-02	1.71e-02
CEC'2013 Functions			
F	CCFR-I ($U = D_i$)	CCFR-I ($U = 2D_i$)	CCFR-I ($U = 10D_i$)
f_1	1.30e-05±3.18e-06	1.40e-05±3.49e-06	1.80e-05±4.65e-06↑
f_2	**5.51e-01±1.47e+00**	5.33e+01±1.70e+01↑	3.14e+02±2.05e+01↑
f_3	2.00e+01±3.06e-07	**2.00e+01±3.23e-07**↓	2.00e+01±3.89e-04↑
f_4	4.50e+07±1.66e+07	5.26e+07±2.22e+07	7.47e+07±2.31e+07↑
f_5	2.53e+06±2.67e+05	2.47e+06±3.75e+05	2.62e+06±3.88e+05
f_6	1.06e+06±1.19e+03	**1.06e+06±1.30e+03**↓	1.07e+06±1.64e+03↑
f_7	8.60e+06±1.90e+07	9.94e+06±2.64e+07	1.04e+07±1.85e+07
f_8	9.61e+09±1.59e+10	9.61e+09±1.59e+10	9.61e+09±1.59e+10
f_9	1.85e+08±2.79e+07	1.84e+08±2.70e+07	1.84e+08±2.73e+07
f_{10}	9.47e+07±1.86e+05	9.46e+07±3.84e+05	**9.43e+07±3.44e+05**↓
f_{11}	3.25e+08±3.24e+08	2.53e+08±3.33e+08	3.28e+08±3.38e+08
f_{12}	6.00e+08±7.09e+08	6.00e+08±7.09e+08	6.00e+08±7.09e+08
f_{13}	9.28e+08±5.33e+08	9.28e+08±5.33e+08	9.28e+08±5.33e+08
f_{14}	2.14e+09±2.11e+09	2.14e+09±2.11e+09	2.14e+09±2.11e+09
f_{15}	8.25e+06±3.28e+06	8.25e+06±3.28e+06	8.25e+06±3.28e+06
R^+	—	49.5	89.5
R^-	—	70.5	30.5
p-value	—	6.25e-01	1.60e-01

The symbols ↑ and ↓ denote that the CCFR-I ($U = D_i$) algorithm performs significantly better than and worse than this algorithm by the Wilcoxon rank sum test at the significance level of 0.05, respectively.

I. Sensitivity Study of the Parameter U of CCFR

Table I summarizes the results of CCFR-I with different values of the parameter U (see Eq. (6a) in the paper) on the CEC'2010 and CEC'2013 large-scale functions [1], [2]. D_i is the dimensionality of the i-th subcomponent.

For the functions with separable variables (i.e., the CEC'2010 functions f_1–f_{13} and the CEC'2013 functions f_1–f_7), the smaller the value of U is, the better the performance of CCFR is in general. This is because CCFR with a small value of U can early stop the evolution of stagnant subpopulations. It can save more computational resources on stagnant variables than CCFR with a larger value of U. Therefore, we use $U = D_i$ as the default setting of U. For the functions without separable variables, the subpopulations hardly enter a stagnant state, so there are no differences between the performance of CCFR-I with different values of U. Overall, the CCFR-I algorithms with different values of U have similar performance on most of the CEC'2010 and CEC'2013 functions.

II. Scalability Study of CCFR

We used the block-rotated ellipsoid function [3] to study the performance of CCFR-I, CBCC1-I, CBCC2-I and CC-I with the scale-up dimensionality of the function and the scale-up number of subcomponents. The dimensionality of the function

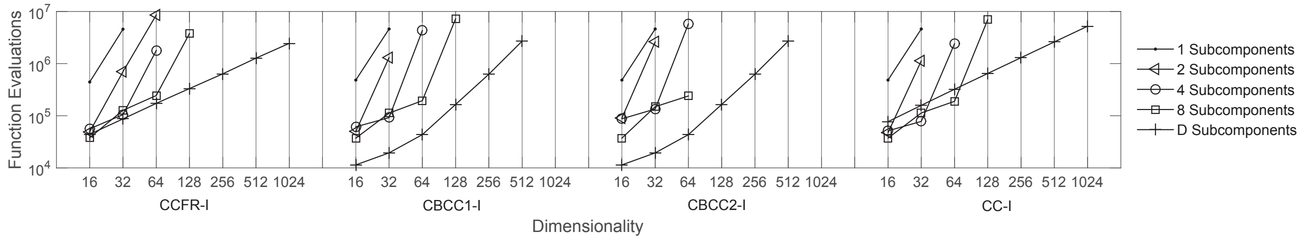

Fig. 1: The average function evaluations used by CCFR-I, CBCC1-I, CBCC2-I and CC-I on the block-rotated ellipsoid function over the successful runs out of 10 runs.

(i.e., D) ranges from 2^4 to 2^{10}. The numbers of subcomponents are $\{1,2,4,8,D\}$. Within 10^7 function evaluations, if the best overall objective value is smaller than a target value (i.e., 0.1) in a run, CCFR-I stops running and this run is considered to be successful. Fig. 1 shows the average number of function evaluations over successful runs out of 10 runs. CCFR-I can reach the target value within 10^7 function evaluations when there are less than 64 variables in a subcomponent. When the number of the variables in a subcomponent is equal to or smaller than eight, the number of function evaluations increases linearly as the dimensionality of the function and the number of subcomponents increase. When there are more than eight variables in a subcomponent, the number of function evaluations increases rapidly and linearly as the dimensionality of the function and the number of subcomponents increase. It can be seen in Fig. 1 that CBCC1-I, CBCC2-I and CC-I have similar performance to CCFR-I, but for CCFR-I, as the dimensionality of the function and the number of subcomponents increase, the number of function evaluations increases less rapidly than the other three CC algorithms.

III. Performance of CCFR with DG and IDG2

In order to study the effect of decomposition on the performance of CCFR, we tested CCFR with two grouping methods (DG [4] and IDG2 [5]). DG is a differential grouping method with a theoretical foundation, which is able to group the interdependent variables together with a high accuracy. In DG, the parameter ϵ was set to 10^{-3}, which is recommended in [4]. IDG2 is an improved variant of DG, which is able to group the interdependent variables together better than DG. Table II summarizes the grouping results of IDG2 and DG.

Table III summarizes the optimization results of CCFR, CBCC1 [6], CBCC2 [6] and DECC [4] with IDG2 and DG. Note that, for the algorithms with IDG2 and DG, the function evaluations spent on groupings (see the 'FEs' column in Table II) are counted as part of the computational budget. The results show that CCFR-IDG2 and CCFR-DG perform better than the other peer algorithms on the CEC'2010 and CEC'2013 functions.

CCFR-DG performs significantly better than the other peer algorithms with DG on most of the separable functions (f_1–f_3). For almost all the partially separable functions (the CEC'2010 functions f_4–f_{18}; the CEC'2013 functions f_4–f_{11}), the differences between the results of the algorithms with DG are not significant. For the CEC'2010 functions f_7, f_8 and f_{13}, because DG is not able to identify the interdependence between variables, there is interdependence between the subcomponents formed by DG. CCFR-DG performs worse than CBCC1-DG and DECC-DG by several orders of magnitude. This indicates that if there is interdependence between subcomponents, optimizing each subcomponent one by one may be a good way.

CCFR-IDG2 outperforms the other peer algorithms on most of the separable and partially separable functions (the CEC'2010 functions f_1–f_{18}; the CEC'2013 functions f_1–f_{11}), especially on the separable functions (f_1–f_3). For the partially separable functions on which CCFR-IDG2 performs worse, the differences between the results of CCFR and the other peer algorithms are not significant. For the functions on which CCFR-IDG2 performs better, the differences are significant. For the nonseparable functions (the CEC'2010 functions f_{19}–f_{20}; the CEC'2013 functions f_{12}–f_{15}), all the variables are grouped into one subcomponent. Therefore, the algorithms with IDG2 have similar performance on these nonseparable functions.

For most of the functions, the algorithms with IDG2 perform better than the ones with DG. This is because IDG2 can identify the interdependence between variables with higher accuracies than DG (see Table II). The results show that compared with DG, IDG2 makes CCFR perform much better than the other peer algorithms. For most of the functions on which CCFR-IDG2 performs worse than CCFR-DG, the performance of CCFR-IDG2 and CCFR-DG does not differ greatly. For most of the functions on which CCFR-IDG2 performs better than CCFR-DG, CCFR-IDG2 significantly outperforms CCFR-DG by several orders of magnitude due to the higher grouping accuracies of IDG2 in identifying the interdependence between variables (e.g., the CEC'2010 functions f_7, f_8, f_{13} and f_{18}; the CEC'2013 functions f_4, f_7, f_8 and f_{11}). The experimental results show that the performance of CCFR is dependent on the decomposition method. A high grouping accuracy can improve the performance of CCFR, especially for the nonseparable variables.

IV. Comparison Between CCFR-IDG2 and Non-CC Algorithms

Table IV summarizes the results of CCFR-IDG2, MA-SW-Chains [7] and MOS-CEC2013 [8]. MA-SW-Chains and MOS-CEC2013 were ranked the first in the IEEE CEC'2010 and CEC'2013 competitions on large-scale global optimization,

TABLE II: The grouping results on the CEC'2010 and CEC'2013 functions. The values of IDG2 and DG are separated by "/". The bold font indicates IDG2 performs better than DG; the gray background indicates IDG2 performs worse than DG.

CEC'2010 Functions

F	Sep Vars	Non-Sep		IDG2 / DG ($\epsilon = 10^{-3}$)						
		Vars	Groups	FEs	Sep			Non-sep		
					Formed Vars	Captured Vars	Accuracy	Formed Subcomponents	Captured Subcomponents	Accuracy
f_1	1000	0	0	500501 / 1001000	1000 / 1000	1000 / 1000	100.0% / 100.0%	0 / 0	0 / 0	100.0% / 100.0%
f_2	1000	0	0	500501 / 1001000	1000 / 1000	1000 / 1000	100.0% / 100.0%	0 / 0	0 / 0	100.0% / 100.0%
f_3	1000	0	0	500501 / 1001000	0 / 1000	0 / 1000	0.0% / 100.0%	1 / 0	0 / 0	100.0% / 100.0%
f_4	950	50	1	500501 / 14554	950 / 33	950 / 33	**100.0% / 3.5%**	1 / 10	1 / 1	100.0% / 100.0%
f_5	950	50	1	500501 / 905450	950 / 950	950 / 950	100.0% / 100.0%	1 / 1	1 / 1	100.0% / 100.0%
f_6	950	50	1	500501 / 906332	854 / 950	854 / 950	89.9% / 100.0%	2 / 1	1 / 1	100.0% / 100.0%
f_7	950	50	1	500501 / 67742	950 / 248	950 / 248	**100.0% / 26.1%**	1 / 4	1 / 0	**100.0% / 0.0%**
f_8	950	50	1	500501 / 23286	950 / 134	950 / 133	**100.0% / 14.0%**	1 / 5	1 / 0	**100.0% / 0.0%**
f_9	500	500	10	500501 / 270802	500 / 500	500 / 500	100.0% / 100.0%	10 / 10	10 / 10	100.0% / 100.0%
f_{10}	500	500	10	500501 / 272958	500 / 500	500 / 500	100.0% / 100.0%	10 / 10	10 / 10	100.0% / 100.0%
f_{11}	500	500	10	500501 / 270640	0 / 501	0 / 500	0.0% / 100.0%	11 / 10	10 / 9	**100.0% / 90.0%**
f_{12}	500	500	10	500501 / 271390	500 / 500	500 / 500	100.0% / 100.0%	10 / 10	10 / 10	100.0% / 100.0%
f_{13}	500	500	10	500501 / 50328	500 / 131	500 / 107	**100.0% / 21.4%**	10 / 34	10 / 0	**100.0% / 0.0%**
f_{14}	0	1000	20	500501 / 21000	0 / 0	0 / 0	100.0% / 100.0%	20 / 20	20 / 20	100.0% / 100.0%
f_{15}	0	1000	20	500501 / 21000	0 / 0	0 / 0	100.0% / 100.0%	20 / 20	20 / 20	100.0% / 100.0%
f_{16}	0	1000	20	500501 / 21128	0 / 4	0 / 0	100.0% / 100.0%	20 / 20	20 / 16	**100.0% / 80.0%**
f_{17}	0	1000	20	500501 / 21000	0 / 0	0 / 0	100.0% / 100.0%	20 / 20	20 / 20	100.0% / 100.0%
f_{18}	0	1000	20	500501 / 39624	0 / 78	0 / 0	100.0% / 100.0%	20 / 50	20 / 0	**100.0% / 0.0%**
f_{19}	0	1000	1	500501 / 2000	0 / 0	0 / 0	100.0% / 100.0%	1 / 1	1 / 1	100.0% / 100.0%
f_{20}	0	1000	1	500501 / 155430	0 / 33	0 / 0	100.0% / 100.0%	1 / 241	1 / 0	**100.0% / 0.0%**

CEC'2013 Functions

F	Sep Vars	Non-Sep		IDG2 / DG ($\epsilon = 10^{-3}$)						
		Vars	Groups	FEs	Sep			Non-sep		
					Formed Vars	Captured Vars	Accuracy	Formed Subcomponents	Captured Subcomponents	Accuracy
f_1	1000	0	0	500501 / 1001000	1000 / 1000	1000 / 1000	100.0% / 100.0%	0 / 0	0 / 0	100.0% / 100.0%
f_2	1000	0	0	500501 / 1001000	1000 / 1000	1000 / 1000	100.0% / 100.0%	0 / 0	0 / 0	100.0% / 100.0%
f_3	1000	0	0	500501 / 1001000	0 / 1000	0 / 1000	0.0% / 100.0%	1 / 0	0 / 0	100.0% / 100.0%
f_4	700	300	7	500501 / 15792	700 / 40	700 / 40	**100.0% / 5.7%**	7 / 13	7 / 3	**100.0% / 58.3%**
f_5	700	300	7	500501 / 527026	700 / 707	700 / 700	100.0% / 100.0%	7 / 10	7 / 6	**100.0% / 66.7%**
f_6	700	300	7	500501 / 579848	0 / 752	0 / 700	0.0% / 100.0%	8 / 5	7 / 3	**100.0% / 50.0%**
f_7	700	300	7	500501 / 11452	700 / 64	700 / 64	**100.0% / 9.1%**	7 / 10	7 / 0	**100.0% / 0.0%**
f_8	0	1000	20	500501 / 22682	200 / 4	0 / 0	100.0% / 100.0%	18 / 25	18 / 14	**80.0% / 65.0%**
f_9	0	1000	20	500501 / 17650	0 / 0	0 / 0	100.0% / 100.0%	20 / 20	20 / 20	100.0% / 100.0%
f_{10}	0	1000	20	500501 / 48650	0 / 152	0 / 0	100.0% / 100.0%	20 / 18	20 / 14	**100.0% / 65.0%**
f_{11}	0	1000	20	500501 / 9102	0 / 1	0 / 0	100.0% / 100.0%	20 / 18	20 / 0	**100.0% / 0.0%**
f_{12}	0	1000	1	500501 / 149894	0 / 50	0 / 0	100.0% / 100.0%	1 / 222	1 / 0	**100.0% / 0.0%**
f_{13}	0	905	1	409966 / 18786	0 / 0	0 / 0	100.0% / 100.0%	1 / 20	1 / 0	**100.0% / 0.0%**
f_{14}	0	905	1	409966 / 26698	0 / 0	0 / 0	100.0% / 100.0%	1 / 19	1 / 0	**100.0% / 0.0%**
f_{15}	0	1000	1	500501 / 2000	0 / 0	0 / 0	100.0% / 100.0%	1 / 1	1 / 1	100.0% / 100.0%

respectively. For the partially separable functions (the CEC'2010 functions f_4–f_{18}; the CEC'2013 functions f_4–f_{11}) on which CCFR-IDG2 performs better than MA-SW-Chains, the differences between the results of CCFR-IDG2 and MA-SW-Chains are significant. For the partially separable functions on which CCFR-IDG2 performs worse than MA-SW-Chains, the differences are not significant except for the CEC'2010 function f_{12}. CCFR-IDG2 performs worse than MOS-CEC2013 on most of the CEC'2010 and CEC'2013 functions. For the nonseparable functions (the CEC'2010 functions f_{19}–f_{20}; the CEC'2013 functions f_{12}–f_{15}), CCFR-IDG2 optimizes all the decision variables together and performs significantly worse than MA-SW-Chains and MOS-CEC2013. This indicates that the optimizer used by CCFR-IDG2 (i.e., SaNSDE) is inferior to MA-SW-Chains and MOS-CEC2013. The results show that CCFR-IDG2 performs worse than MA-SW-Chains and MOS-CEC2013 on the CEC'2013 functions. This may be because that the optimizer used by CCFR-IDG2 performs worse than MA-SW-Chains and MOS-CEC2013. The previous experimental results have shown that for a given optimizer (i.e., SaNSDE), CCFR is superior to the other peer algorithms with the same optimizer.

Fig. 2 shows the convergence of CCFR-IDG2, MA-SW-Chains and MOS-CEC2013. Because CCFR-IDG2 spends 500501 function evaluations grouping the decision variables, in Fig. 2 the convergence lines of CCFR-IDG2 start from 500502 function evaluations. For separable function f_1, CCFR-IDG2 optimizes each separable variable one by one and converges slowly, but when CCFR-IDG2 finishes optimizing the last variable with the largest weight value, the best overall objective value drops sharply. f_8 is a partially separable function with imbalance between subcomponents. For f_8, compared with MA-SW-Chains and MOS-CEC2013, in the beginning of the evolutionary process, CCFR-IDG2 converges very slowly. When the first evolutionary cycle ends (about 0.8×10^6 function evaluations), CCFR-IDG2 starts to select the subpopulation with the greatest contribution

TABLE III: The average fitness values ± standard deviations on the CEC'2010 and CEC'2013 functions over 25 independent runs. The significantly better results are in bold font (Wilcoxon rank sum test with Holm p-value correction, α=0.05). R^+, R^- and p-value have similar meanings as in Table I.

CEC'2010 Functions								
F	CCFR-IDG2	CBCC1-IDG2	CBCC2-IDG2	DECC-IDG2	CCFR-DG	CBCC1-DG	CBCC2-DG	DECC-DG
f_1	**1.6e-05±6.5e-06**	1.7e+07±2.1e+07↑	1.7e+07±2.1e+07↑	1.7e+07±2.1e+07↑	4.8e+08±9.8e+07	2.9e+07±3.1e+07↓	2.9e+07±3.1e+07↓	2.9e+07±3.1e+07↓
f_2	**1.7e+02±8.6e+00**	4.7e+03±4.8e+02↑	4.7e+03±4.8e+02↑	4.7e+03±4.8e+02↑	**3.2e+02±1.7e+01**	4.7e+03±4.8e+02↑	4.7e+03±4.8e+02↑	4.7e+03±4.8e+02↑
f_3	1.2e+01±3.7e-01	1.2e+01±3.7e-01	1.2e+01±3.7e-01	1.2e+01±3.7e-01	**1.1e+01±3.8e-01**	1.2e+01±3.7e-01↑	1.2e+01±3.7e-01↑	1.2e+01±3.7e-01↑
f_4	1.3e+11±7.5e+10	7.4e+10±4.8e+10↓	1.1e+11±2.9e+10	8.9e+10±4.6e+10↓	4.3e+10±1.6e+10	3.5e+11±2.0e+11↑	5.1e+10±3.1e+10	7.8e+11±5.5e+11↑
f_5	9.2e+07±1.6e+07	6.8e+07±1.1e+07↓	6.8e+07±9.4e+06↓	6.7e+07±1.0e+07↓	4.9e+08±2.4e+07	6.9e+07±1.0e+07↓	6.9e+07±1.0e+07↓	6.9e+07±1.1e+07↓
f_6	6.8e+05±7.1e+05	1.1e+06±7.9e+05↑	1.1e+06±6.9e+05↑	6.4e+05±6.8e+05	1.1e+07±7.5e+05	1.3e+06±6.4e+05↓	1.3e+06±6.4e+05↓	**8.1e+05±7.2e+05**↓
f_7	**2.0e-03±3.5e-04**	7.9e+04±1.0e+04↑	1.1e+05±1.8e+04↑	4.2e+04±1.2e+04↑	2.7e+07±7.0e+07	1.1e+05±8.5e+04↓	7.6e+09±6.6e+09↑	**6.0e+04±3.3e+04**↓
f_8	**3.2e+05±1.1e+06**	8.8e+05±1.6e+06↑	1.1e+06±1.7e+06↑	5.2e+05±1.3e+06↑	2.6e+08±1.9e+08	**4.6e+06±8.8e+06**↓	6.3e+07±6.0e+07↓	1.5e+07±2.3e+07↓
f_9	1.3e+07±1.7e+06	2.1e+07±2.2e+07	4.4e+09±7.0e+08↑	5.4e+07±6.4e+07↑	1.1e+07±1.4e+06	1.8e+07±2.1e+07	1.8e+07±2.1e+07	3.3e+07±2.0e+07↑
f_{10}	**1.8e+03±1.4e+02**	3.4e+03±1.7e+02↑	4.6e+03±7.7e+02↑	4.3e+03±1.8e+02↑	**1.6e+03±1.2e+02**	3.2e+03±1.7e+02↑	3.2e+03±1.7e+02↑	4.1e+03±1.7e+02↑
f_{11}	**2.0e+01±3.3e+00**	2.4e+01±2.4e+00↑	2.5e+01±2.3e+00↑	2.3e+01±2.1e+00↑	**1.1e+01±2.5e+00**	2.3e+01±2.2e+00↑	2.3e+01±2.1e+00↑	2.3e+01±2.7e+00↑
f_{12}	**2.0e+01±2.2e+01**	2.6e+04±7.4e+03↑	3.7e+04±9.7e+03↑	2.3e+04±8.8e+03↑	**4.6e+00±6.9e+00**	2.2e+04±6.3e+03↑	2.2e+04±6.3e+03↑	1.9e+04±7.3e+03↑
f_{13}	**5.3e+02±1.0e+02**	2.6e+04±7.8e+03↑	3.9e+04±6.2e+03↑	2.5e+04±7.8e+03↑	2.8e+06±9.2e+05	**5.8e+03±4.4e+03**↓	1.6e+04±7.8e+03↓	8.7e+03±3.9e+03↓
f_{14}	**3.1e+07±3.3e+06**	3.5e+07±2.6e+06↑	9.5e+09±5.2e+08↑	3.3e+07±2.7e+06↑	**2.5e+07±2.9e+06**	2.8e+07±2.1e+06↑	2.8e+07±2.1e+06↑	2.7e+07±2.2e+06↑
f_{15}	**3.2e+03±1.5e+02**	4.4e+03±1.5e+02↑	4.6e+03±1.7e+02↑	4.4e+03±1.9e+02↑	**2.8e+03±1.3e+02**	4.0e+03±1.5e+02↑	4.0e+03±1.5e+02↑	4.0e+03±1.6e+02↑
f_{16}	2.0e+01±2.6e+00	1.9e+01±3.2e+00	2.0e+01±3.4e+00	2.0e+01±4.0e+00	2.4e+01±4.3e+00	2.0e+01±3.4e+00↓	2.1e+01±3.1e+00	2.1e+01±3.4e+00
f_{17}	**6.7e+01±8.7e+01**	1.3e+02±8.9e+01↑	7.2e+02±3.4e+02↑	8.0e+01±5.2e+01↑	1.1e+01±1.1e+01	3.6e+01±4.9e+01↑	3.6e+01±4.9e+01↑	2.4e+01±3.7e+01
f_{18}	1.4e+03±1.9e+02	1.3e+03±1.9e+02	1.7e+03±2.4e+02↑	1.2e+03±1.5e+02↓	**1.3e+08±9.9e+07**	6.9e+09±2.3e+09↑	1.4e+10±2.0e+09↑	2.1e+10±3.9e+09↑
f_{19}	1.3e+06±1.0e+05	1.3e+06±1.0e+05	1.3e+06±1.0e+05	1.3e+06±1.0e+05	1.2e+06±9.5e+04	1.2e+06±9.5e+04	1.2e+06±9.5e+04	1.2e+06±9.5e+04
f_{20}	2.0e+09±1.8e+09	2.0e+09±1.8e+09	2.0e+09±1.8e+09	2.0e+09±1.8e+09	**3.1e+07±6.6e+06**	1.4e+10±2.7e+09↑	1.6e+08±1.5e+08↑	3.3e+10±5.9e+09↑
R^+	—	165.0	174.0	153.0	—	123.0	137.0	123.0
R^-	—	45.0	36.0	57.0	—	87.0	73.0	87.0
p-value	—	2.51e-02	1.00e-02	7.31e-02	—	5.02e-01	2.32e-01	5.02e-01
CEC'2013 Functions								
F	CCFR-IDG2	CBCC1-IDG2	CBCC2-IDG2	DECC-IDG2	CCFR-DG	CBCC1-DG	CBCC2-DG	DECC-DG
f_1	**1.8e-05±4.5e-06**	4.6e+07±1.3e+08↑	4.6e+07±1.3e+08↑	4.6e+07±1.3e+08↑	4.8e+08±6.9e+07	6.2e+07±1.3e+08↓	6.2e+07±1.3e+08↓	6.2e+07±1.3e+08↓
f_2	**3.6e+02±2.1e+01**	2.1e+04±1.0e+03↑	2.1e+04±1.0e+03↑	2.1e+04±1.0e+03↑	**7.4e+02±4.0e+01**	2.1e+04±1.0e+03↑	2.1e+04±1.0e+03↑	2.1e+04±1.0e+03↑
f_3	2.1e+01±1.2e-02	2.1e+01±1.2e-02	2.1e+01±1.2e-02	2.1e+01±1.2e-02	**2.0e+01±6.0e-07**	2.1e+01±1.1e-02↑	2.1e+01±1.1e-02↑	2.1e+01±1.1e-02↑
f_4	**9.6e+07±4.0e+07**	2.2e+08±6.0e+07↑	6.6e+10±5.6e+09↑	2.9e+08±9.7e+07↑	9.1e+10±5.6e+10	8.7e+10±5.1e+10	4.6e+11±2.8e+11↑	8.3e+10±4.7e+10
f_5	2.8e+06±3.2e+05	2.6e+06±4.3e+05	2.5e+06±4.7e+05↓	3.0e+06±4.7e+05	3.0e+06±5.2e+05	2.8e+06±3.6e+05	2.6e+06±4.4e+05↓	3.3e+06±4.0e+05↑
f_6	1.1e+06±1.0e+03	1.1e+06±1.7e+03↓	1.1e+06±1.8e+03↓	1.1e+06±1.6e+03↓	1.1e+06±1.6e+03	1.1e+06±2.1e+03↓	1.1e+06±1.5e+03↓	1.1e+06±2.3e+03↓
f_7	2.0e+07±2.9e+07	2.2e+07±2.6e+07	9.9e+07±3.7e+08	2.4e+07±3.8e+07	1.4e+08±9.7e+07	1.2e+08±3.9e+07	1.6e+10±1.4e+10↑	1.4e+08±7.1e+07
f_8	**6.6e+10±9.5e+10**	2.3e+13±1.6e+13↑	1.1e+12±1.7e+11↑	7.4e+13±5.8e+13↑	1.6e+15±1.0e+15	2.0e+15±1.5e+15	5.9e+15±4.3e+15↑	2.0e+15±1.4e+15
f_9	**1.9e+08±2.8e+07**	2.6e+08±4.0e+07↑	2.3e+08±3.0e+07↑	3.0e+08±5.7e+07↑	**1.9e+08±2.8e+07**	2.5e+08±3.8e+07↑	2.2e+08±2.9e+07↑	2.9e+08±5.2e+07↑
f_{10}	9.5e+07±1.8e+05	9.4e+07±2.8e+05↓	9.4e+07±2.5e+05↓	9.5e+07±3.0e+05↓	9.5e+07±3.1e+05	9.4e+07±6.1e+05↓	9.4e+07±6.6e+05↓	9.4e+07±2.4e+05↓
f_{11}	4.2e+08±3.4e+08	5.0e+09±1.5e+10	7.3e+10±1.2e+11↑	2.8e+09±1.1e+10	**2.8e+10±6.0e+10**	4.5e+10±6.1e+10↑	5.2e+12±3.7e+12↑	4.7e+10±5.7e+10↑
f_{12}	1.6e+09±1.6e+09	1.6e+09±1.6e+09	1.6e+09±1.6e+09	1.6e+09±1.6e+09	**8.0e+07±8.3e+06**	6.0e+10±8.3e+09↑	6.6e+08±1.3e+08↑	1.2e+11±1.4e+10↑
f_{13}	1.2e+09±6.0e+08	1.2e+09±6.0e+08	1.2e+09±6.0e+08	1.2e+09±6.0e+08	**2.0e+09±1.0e+09**	4.0e+09±1.5e+09↑	4.1e+10±2.7e+10↑	6.3e+09±1.9e+09↑
f_{14}	3.4e+09±3.1e+09	3.5e+09±3.2e+09	3.5e+09±3.2e+09	3.5e+09±3.2e+09	7.4e+09±8.5e+09	1.3e+10±1.2e+10↑	5.0e+11±1.2e+12↑	8.9e+09±6.8e+09
f_{15}	9.8e+06±3.7e+06	9.9e+06±3.7e+06	9.9e+06±3.7e+06	9.9e+06±3.7e+06	8.3e+06±3.3e+06	8.3e+06±3.3e+06	8.3e+06±3.3e+06	8.3e+06±3.3e+06
R^+	—	107.0	107.0	112.0	—	80.0	99.0	91.0
R^-	—	13.0	13.0	8.0	—	40.0	21.0	29.0
p-value	—	5.37e-03	5.37e-03	1.53e-03	—	2.77e-01	2.56e-02	8.33e-02

The symbols ↑ and ↓ have similar meanings as in Table I.

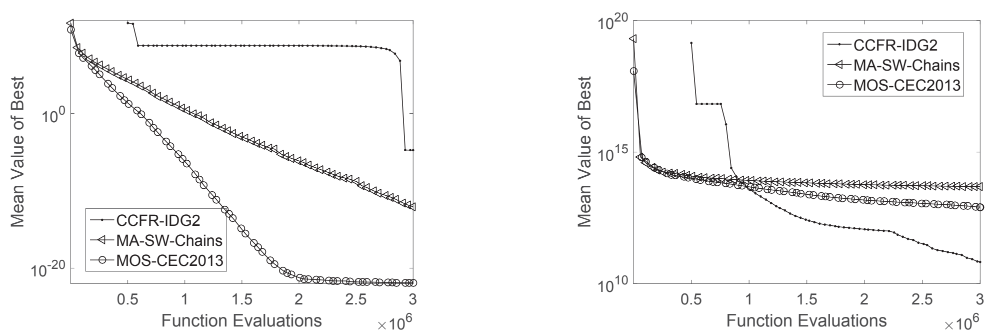

(a) f_1 (b) f_8

Fig. 2: The average convergence on two selected CEC'2013 functions over 25 independent runs.

to undergo evolution. CCFR-IDG2 then converges much faster than MA-SW-Chains and MOS-CEC2013. This indicates that if the optimizer used by CCFR-IDG2 performs well on a function, CCFR might outperform MA-SW-Chains and MOS-CEC2013 on that function.

To improve the performance of CCFR-IDG2, we replaced SaNSDE with CMAES [9]. Table V summarizes the results of CCFR-IDG2 with CMAES. CCFR-IDG2 with CMAES significantly outperforms MA-SW-Chains on almost all the CEC'2010 and CEC'2013 functions. CCFR-IDG2 with CMAES performs significantly better than MOS-CEC2013 by several orders of magnitude on most of the partially separable functions (the CEC'2010 functions f_4–f_{18}; the CEC'2013 functions f_4–f_{11}).

TABLE IV: The average errors ± standard deviations on the CEC'2010 and CEC'2013 functions over 25 independent runs. The significantly better results are in bold font (Wilcoxon rank sum test with Holm p-value correction, α=0.05). R^+, R^- and p-value have similar meanings as in Table I.

CEC'2010 Functions			
F	CCFR-IDG2	MA-SW-Chains	MOS-CEC2013
f_1	1.62e-05±6.55e-06	3.88e-14±3.59e-14↓	**0.00e+00±0.00e+00**↓
f_2	1.73e+02±8.62e+00	8.63e+02±5.84e+01↑	**0.00e+00±0.00e+00**↓
f_3	1.22e+01±3.66e-01	**5.41e-13±2.13e-13**↓	1.65e-12±6.73e-14↓
f_4	1.26e+11±7.50e+10	2.94e+11±9.32e+10↑	**1.56e+10±6.02e+09**↓
f_5	**9.15e+07±1.61e+07**	1.75e+08±1.03e+08↑	1.11e+08±2.25e+07↑
f_6	6.85e+05±7.05e+05	3.52e+04±1.72e+05	**1.22e-07±6.43e-08**↓
f_7	2.04e-03±3.45e-04	3.30e+02±1.40e+03	**0.00e+00±0.00e+00**↓
f_8	3.19e+05±1.08e+06	9.28e+06±2.36e+07↑	**1.95e+00±8.03e+00**↓
f_9	1.34e+07±1.68e+06	1.45e+07±1.59e+06	**3.46e+06±4.49e+05**↓
f_{10}	**1.81e+03±1.43e+02**	2.06e+03±1.19e+02↑	3.78e+03±1.47e+02↑
f_{11}	**1.99e+01±3.26e+00**	3.69e+01±8.24e+00↑	1.91e+02±4.07e-01↑
f_{12}	2.03e+01±2.23e+01	3.19e-06±5.32e-07↓	**0.00e+00±0.00e+00**↓
f_{13}	5.26e+02±1.04e+02	1.09e+03±6.29e+02↑	7.14e+02±5.68e+02
f_{14}	3.08e+07±3.35e+06	3.34e+07±3.37e+06↑	**9.80e+06±6.03e+05**↓
f_{15}	3.18e+03±1.51e+02	**2.69e+03±9.75e+01**↓	7.44e+03±1.84e+02↑
f_{16}	**2.01e+01±2.62e+00**	1.08e+02±1.51e+01↑	3.82e+02±1.55e+01↑
f_{17}	6.72e+01±8.68e+01	1.26e+00±9.45e-02↓	**2.83e-07±7.97e-08**↓
f_{18}	1.37e+03±1.93e+02	1.87e+03±5.79e+02↑	1.54e+03±7.46e+02
f_{19}	1.28e+06±1.01e+05	2.85e+05±1.74e+04↓	**2.91e+04±2.14e+03**↓
f_{20}	1.97e+09±1.83e+09	1.05e+03±7.59e+01↓	**3.52e+02±4.43e+02**↓
R^+	—	143.0	73.0
R^-	—	67.0	137.0
p-value	—	1.56e-01	2.32e-01
CEC'2013 Functions			
F	CCFR-IDG2	MA-SW-Chains	MOS-CEC2013
f_1	1.77e-05±4.52e-06	8.49e-13±1.09e-12↓	**1.27e-22±7.41e-23**↓
f_2	**3.64e+02±2.06e+01**	1.22e+03±1.14e+02↑	8.32e+02±4.48e+01↑
f_3	2.07e+01±1.21e-02	2.14e+01±5.62e-02↑	**9.18e-13±5.12e-14**↓
f_4	**9.56e+07±4.03e+07**	4.58e+09±2.46e+09↑	1.74e+08±7.87e+07↑
f_5	2.80e+06±3.18e+05	**1.87e+06±3.06e+05**↓	6.94e+06±8.85e+05↑
f_6	1.06e+06±1.05e+03	1.01e+06±1.53e+04↓	**1.48e+05±6.43e+04**↓
f_7	2.03e+07±2.94e+07	3.45e+06±1.27e+06	**1.62e+04±9.10e+03**↓
f_8	**6.63e+10±9.52e+10**	4.85e+13±1.02e+13↑	8.00e+12±3.07e+12↑
f_9	1.89e+08±2.83e+07	**1.07e+08±1.68e+07**↓	3.83e+08±6.29e+07↑
f_{10}	9.48e+07±1.82e+05	9.18e+07±1.06e+06↓	**9.02e+05±5.07e+05**↓
f_{11}	4.17e+08±3.43e+08	2.19e+08±2.98e+07	**5.22e+07±2.05e+07**↓
f_{12}	1.56e+09±1.58e+09	1.25e+03±1.05e+02↓	**2.47e+02±2.54e+02**↓
f_{13}	1.21e+09±6.00e+08	1.98e+07±1.82e+06↓	**3.40e+06±1.06e+06**↓
f_{14}	3.39e+09±3.06e+09	1.36e+08±2.11e+07↓	**2.56e+07±7.94e+06**↓
f_{15}	9.82e+06±3.69e+06	5.71e+06±7.57e+05↓	**2.35e+06±1.94e+05**↓
R^+	—	34.0	41.0
R^-	—	86.0	79.0
p-value	—	1.51e-01	3.03e-01

The symbols ↑ and ↓ have similar meanings as in Table I.

REFERENCES

[1] K. Tang, X. Li, P. N. Suganthan, Z. Yang, and T. Weise, "Benchmark functions for the CEC'2010 special session and competition on large-scale global optimization," Nature Inspired Computation and Applications Laboratory, Tech. Rep., 2010.

[2] X. Li, K. Tang, M. N. Omidvar, Z. Yang, and K. Qin, "Benchmark functions for the CEC'2013 special session and competition on large scale global optimization," Evolutionary Computation and Machine Learning Group, RMIT University, Australia, Tech. Rep., 2013.

[3] R. Ros and N. Hansen, "A simple modification in cma-es achieving linear time and space complexity," in *Parallel Problem Solving from Nature*, 2008, pp. 296–305.

[4] M. N. Omidvar, X. Li, Y. Mei, and X. Yao, "Cooperative co-evolution with differential grouping for large scale optimization," *IEEE Transactions on Evolutionary Computation*, vol. 18, no. 3, pp. 378–393, 2014.

[5] M. N. Omidvar, M. Yang, Y. Mei, X. Li, and X. Yao, "IDG: A faster and more accurate differential grouping algorithm," University of Birmingham, School of Computer Science, Tech. Rep. CSR-15-04, September 2015. [Online]. Available: ftp://ftp.cs.bham.ac.uk/pub/tech-reports/2015/CSR-15-04.pdf

[6] M. N. Omidvar, X. Li, and X. Yao, "Smart use of computational resources based on contribution for cooperative co-evolutionary algorithms," in *Genetic and Evolutionary Computation Conference*, 2011, pp. 1115–1122.

[7] D. Molina, M. Lozano, and F. Herrera, "MA-SW-Chains: Memetic algorithm based on local search chains for large scale continuous global optimization," in *IEEE Congress on Evolutionary Computation*, 2010, pp. 1–8.

[8] A. LaTorre, S. Muelas, and J.-M. Pena, "Large scale global optimization: Experimental results with mos-based hybrid algorithms," in *IEEE Congress on Evolutionary Computation*, 2013, pp. 2742–2749.

[9] N. Hansen, S. D. Müller, and P. Koumoutsakos, "Reducing the time complexity of the derandomized evolution strategy with covariance matrix adaptation (cma-es)," *Evol. Comput.*, vol. 11, no. 1, pp. 1–18, 2003.

TABLE V: The average errors ± standard deviations on the CEC'2010 and CEC'2013 functions over 25 independent runs. The significantly better results are in bold font (Wilcoxon rank sum test with Holm p-value correction, α=0.05). R^+, R^- and p-value have similar meanings as in Table I.

CEC'2010 Functions			
F	CCFR-IDG2 (CMAES)	MA-SW-Chains	MOS-CEC2013
f_1	5.50e-17±2.15e-17	3.88e-14±3.59e-14↑	**0.00e+00±0.00e+00**↓
f_2	5.41e+02±4.80e+01	8.63e+02±5.84e+01↑	**0.00e+00±0.00e+00**↓
f_3	1.02e+00±3.98e-01	**5.41e-13±2.13e-13**↓	1.65e-12±6.73e-14↓
f_4	**4.28e-03±4.98e-03**	2.94e+11±9.32e+10↑	1.56e+10±6.02e+09↑
f_5	1.10e+08±1.60e+07	1.75e+08±1.03e+08↑	1.11e+08±2.25e+07
f_6	9.58e+00±8.51e-01	3.52e+04±1.72e+05↑	**1.22e-07±6.43e-08**↓
f_7	4.47e-07±1.73e-06	3.30e+02±1.40e+03↑	**0.00e+00±0.00e+00**↓
f_8	1.25e+06±1.85e+06	9.28e+06±2.36e+07↑	1.95e+00±8.03e+00
f_9	**9.28e-06±5.47e-06**	1.45e+07±1.59e+06↑	3.46e+06±4.49e+05↑
f_{10}	**1.29e+03±6.14e+01**	2.06e+03±1.19e+02↑	3.78e+03±1.47e+02↑
f_{11}	**2.35e-01±4.08e-01**	3.69e+01±8.24e+00↑	1.91e+02±4.07e-01↑
f_{12}	1.28e-10±9.64e-11	3.19e-06±5.32e-07↑	**0.00e+00±0.00e+00**↓
f_{13}	**4.73e+00±3.79e+00**	1.09e+03±6.29e+02↑	7.14e+02±5.68e+02↑
f_{14}	**2.61e-19±3.26e-20**	3.34e+07±3.37e+06↑	9.80e+06±6.03e+05↑
f_{15}	**2.04e+03±8.22e+01**	2.69e+03±9.75e+01↑	7.44e+03±1.84e+02↑
f_{16}	**8.07e-13±2.60e-14**	1.08e+02±1.51e+01↑	3.82e+02±1.55e+01↑
f_{17}	**7.42e-24±1.63e-25**	1.26e+00±9.45e-02↑	2.83e-07±7.97e-08↑
f_{18}	**1.09e+01±6.87e+00**	1.87e+03±5.79e+02↑	1.54e+03±7.46e+02↑
f_{19}	**2.12e+04±2.21e+03**	2.85e+05±1.74e+04↑	2.91e+04±2.14e+03↑
f_{20}	8.50e+02±2.50e+01	1.05e+03±7.59e+01↑	**3.52e+02±4.43e+02**↓
R^+	—	207.0	157.0
R^-	—	3.0	53.0
p-value	—	1.40e-04	5.22e-02
CEC'2013 Functions			
F	CCFR-IDG2 (CMAES)	MA-SW-Chains	MOS-CEC2013
f_1	5.52e-17±5.70e-18	8.49e-13±1.09e-12↑	**1.27e-22±7.41e-23**↓
f_2	**4.35e+02±3.55e+01**	1.22e+03±1.14e+02↑	8.32e+02±4.48e+01↑
f_3	2.04e+01±5.30e-02	2.14e+01±5.62e-02↑	**9.18e-13±5.12e-14**↓
f_4	**5.58e+03±2.73e+04**	4.58e+09±2.46e+09↑	1.74e+08±7.87e+07↑
f_5	2.19e+06±3.11e+05	**1.87e+06±3.06e+05**↓	6.94e+06±8.85e+05↑
f_6	9.99e+05±1.26e+04	1.01e+06±1.53e+04↑	**1.48e+05±6.43e+04**↓
f_7	**2.22e-08±4.21e-08**	3.45e+06±1.27e+06↑	1.62e+04±9.10e+03↑
f_8	**4.89e+03±1.23e+03**	4.85e+13±1.02e+13↑	8.00e+12±3.07e+12↑
f_9	1.59e+08±3.33e+07	**1.07e+08±1.68e+07**↓	3.83e+08±6.29e+07↑
f_{10}	9.11e+07±1.35e+06	9.18e+07±1.06e+06↑	**9.02e+05±5.07e+05**↓
f_{11}	**4.64e-05±7.47e-05**	2.19e+08±2.98e+07↑	5.22e+07±2.05e+07↑
f_{12}	1.01e+03±5.20e+01	1.25e+03±1.05e+02↑	**2.47e+02±2.54e+02**↓
f_{13}	**2.58e+06±3.00e+05**	1.98e+07±1.82e+06↑	3.40e+06±1.06e+06↑
f_{14}	3.63e+07±3.21e+06	1.36e+08±2.11e+07↑	**2.56e+07±7.94e+06**↓
f_{15}	2.80e+06±2.77e+05	5.71e+06±7.57e+05↑	**2.35e+06±1.94e+05**↓
R^+	—	103.0	77.0
R^-	—	17.0	43.0
p-value	—	1.25e-02	3.59e-01

The symbols ↑ and ↓ have similar meanings as in Table I.